



Formation of mixed Al–Fe colloidal sorbent and dissolved-colloidal partitioning of Cu and Zn in the Cement Creek – Animas River Confluence, Silverton, Colorado

Laurence E. Schemel^{a,*}, Briant A. Kimball^b, Robert L. Runkel^c, Marisa H. Cox^a

^a US Geological Survey, Water Resources Division, 345 Middlefield Road, MS 439, Menlo Park, CA 94025, USA

^b US Geological Survey, Water Resources Division, 2329 Orton Circle, Salt Lake City, UT 84119-2047, USA

^c US Geological Survey, Water Resources Division, Denver Federal Center, MS 415, Lakewood, CO 80225, USA

Received 8 August 2006; accepted 20 February 2007

Editorial handling by R. Fuge

Available online 21 March 2007

Abstract

Transport and chemical transformations of dissolved and colloidal Al, Fe, Cu and Zn were studied by detailed sampling in the mixing zone downstream from the confluence of Cement Creek (pH 4.1) with the Animas River (pH 7.6). Complete mixing resulted in circumneutral pH in the downstream reach of the 1300 m study area. All four metals were transported through this mixing zone without significant losses to the streambed, and they exhibited transformations from dissolved to colloidal forms to varying degrees during the mixing process. Nearly all of the Al formed colloidal hydrous Al oxides (HAO) as pH increased (4.8–6.5), whereas colloidal hydrous Fe oxides (HFO) were supplied by Cement Creek as well as formed in the mixing zone primarily at higher pH (>6.5). The short travel time through the mixing zone (approx. 40 min) and pH limited the formation of HFO from dissolved Fe²⁺ supplied by Cement Creek. Although the proportions of HAO and HFO varied as the streams mixed, the colloidal sorbent typically was enriched in HAO relative to HFO by a factor of 1.5–2.1 (by mole) in the pH range where dissolved-to-colloidal partitioning of Cu and Zn was observed. Model simulations of sorption by HFO (alone) greatly underestimated the dissolved-to-colloidal partitioning of Zn. Previous studies have shown that HAO–HFO mixtures can sorb greater amounts of Zn than HFO alone, but the high Zn-to-sorbent ratio in this mixing zone could also account for greater partitioning. In contrast to Zn, comparisons with model simulations did not show that Cu sorption was greater than that for HFO alone, and also indicated that sorption was possibly less than what would be expected for a non-interactive mixture of these two sorbents. These field results for Cu, however, might be influenced by (organic) complexation or other factors in this natural system. Laboratory mixing experiments using natural source waters (upstream of the confluence) showed that the presence of HFO in the mixed sorbent resulted in greater Cu partitioning than for HAO alone, and that the effect was greater with increasing (mole fraction) HFO. This was consistent with field results that showed greater Cu sorption when additional HFO was formed in the downstream reach of the mixing zone. Further research is needed to identify the significance of surface-related mechanisms specific to HAO–HFO mixtures that could affect the partitioning of Cu in natural systems.

Published by Elsevier Ltd.

* Corresponding author. Tel.: +1 650 329 4436; fax: +1 650 329 4327.

E-mail address: lschemel@usgs.gov (L.E. Schemel).

1. Introduction

The chemistry of acidic, surface-water drainage from mines and mineral deposits (AMD) changes or evolves as it travels downstream because of reactions that form insoluble products and mixing with inflows that dilute concentrations and neutralize the acid (Chapman et al., 1983; Berger et al., 2000). During this “natural attenuation” process, Fe and Al commonly form insoluble hydrous oxides, which can be initially transported as micron- and smaller-sized particles (colloids; Ranville and Schmiermund, 1999) before a combination of chemical, physical and biological processes promote retention by the streambed. Concentrations of other metals, such as Cu and Zn, also can be attenuated because of the sorbent properties of Fe and Al precipitates. Precipitation and sorption, however, are both pH dependent, and in the case of Fe, also time dependent. The oxidation of sulfide minerals produces (soluble) Fe^{2+} , SO_4 , and acid that in turn dissolves other minerals (Nordstrom and Alpers, 1999). Abiotic oxidation to Fe^{3+} , which forms largely insoluble hydrous oxides over a wide pH range (Fox, 1988), is slow at $\text{pH} < 4$, but increases substantially at higher pH and when influenced by microorganisms (Singer and Stumm, 1970). Ferric iron can precipitate at $\text{pH} < 4$, whereas Al precipitates over a higher pH range (4.5–6.5). Therefore, streams affected by AMD can lose Fe to the streambed over time (and distance downstream) while most of the Al remains dissolved. When the stream is neutralized, the relative abundances of Fe and Al in the precipitated colloids will depend on supply to the stream, in-stream oxidation, and retention by the streambed (e.g., Lee et al., 2002; Dinelli and Tateo, 2002). Therefore, mixed colloidal sorbents exhibiting a wide range of Fe and Al composition can be formed in confluences where streams affected by AMD are neutralized.

Laboratory studies of Cu and Zn sorption are typically limited to relatively simple, single-sorbent systems, and field studies most often involve sorbents in the water column or on the streambed that are enriched in a single sorbent relative to others (Smith, 1999, and references therein). Even when mixtures of Fe and Al sorbents occur in field studies, it is often assumed that the stronger sorbent, an Fe hydrous oxide (or oxyhydroxysulfate), will account for most of the sorption. Laboratory studies of binary Fe–Al sorbent mixtures, however, have shown that the two sorbents are interactive, and

that effects on sorption properties can vary greatly among sorbates (Anderson and Benjamin, 1990a,b). For example, sorption of Zn is enhanced when Fe sorbent is enriched in Al sorbent, whereas sorption of Ag and Cd is inhibited. Similarly, X-ray absorption near edge structure spectroscopy has shown that interactions of ferrihydrite with non-crystalline Al hydroxide inhibit phosphate sorption (Khare et al., 2005). In addition to changing other properties of an Fe sorbent, Al hydrous oxides tend to coat other sorbent particles, therefore changing the fundamental nature of the adsorbing surface (Anderson and Benjamin, 1990a). For example, the tendency of Al hydroxide to coat SiO_2 and enhance sorption of Cd and Ca has been reported in laboratory studies (Meng and Letterman, 1993), and field studies have shown that similar coatings containing Fe and Al enhance the sorption of Zn onto aquifer quartz sands (Coston et al., 1995; Davis et al., 1998). Therefore, the above studies show that interactions between Al and Fe hydrous oxides are likely to produce mixtures with sorbent properties that are not directly additive, as might be expected for simple mixtures of independent sorbents.

The main objective of this study is to provide detailed information on the formation and sorption properties of an Fe–Al mixed sorbent produced within a natural stream confluence that is affected by AMD. Field samples were obtained incrementally across multiple sections of the mixing zone to cover the wide range of chemical gradients and resolve changes in the composition of the sorbent and concentrations of dissolved and colloidal Cu and Zn as the streams mixed. Effects of chemical transformations, dilution, dissolved-to-colloidal partitioning, and sorbate-to-sorbent ratio were identified and evaluated. Supporting laboratory experiments were conducted with natural source waters from the two streams to examine effects of mixed sorbent composition primarily on the sorption of Cu. Results from this study were also used to confirm findings from an earlier study that total Al, Fe and Zn were transported conservatively through this confluence (Schemel et al., 2000) and add new information on Cu transport.

2. Study area

The Silverton caldera, which is located in the high-elevation San Juan mountains of southwestern Colorado, was an area of intense mining pri-

marily for Au and Ag for over a century (Baars, 1992; Yager and Bove, 2002; Fig. 1). Generation of metal-rich, acidic water comes from oxidation of abundant sulfides in regionally altered acid-sulfate rocks and quartz-sericite-pyrite mineralized veins from multiple hydrothermal alteration and mineralization events from about 27 Ma to 10 Ma before present (Bove et al., 2001; Lipman et al., 1976). Drainage from numerous inactive mines and altered bedrock continue to supply dissolved and colloidal metals to Cement Creek upstream from the gauging station (Fig. 1; Church et al., 1997; Kimball et al., 2007). Cement Creek (typically $\text{pH} < 4$) flows into the Animas River ($\text{pH} > 7$) near the town of Silverton, creating a mixing zone where products of chemical (neutralization) reactions are clearly evident in the water and on the streambed (Schemel et al., 2000; Schemel and Cox, 2005).

Acidic waters and metals are supplied to the Animas River upstream of Silverton, but neutralization, precipitation and streambed-retention processes largely remove Al and Fe from the riverflow and reduce concentrations of other metals, such as Cu and Zn (Paschke et al., 2005). Similarly, in Cement Creek upstream from the confluence with the Animas River, these processes reduce the total loads

of Al, Fe, Cu and Zn by about half (Kimball et al., 2002). Iron is removed to a greater degree than Al, which is in part due to continuous in-stream oxidation and the precipitation of Fe^{3+} in the acidic streamflow. Similarly, removal of Cu is greater relative to Zn probably because it sorbs to Fe and Al precipitates over a lower pH range. Largest losses, however, occur in reaches affected by inflows from circumneutral streams, where all four metals are removed (Kimball et al., 2002). By the time Cement Creek flow is neutralized in the Animas River confluence, the mixed Al-Fe colloidal sorbent that is formed is enriched in Al by nearly a factor of two by mole (Church et al., 1997; Schemel et al., 2000).

Physical and hydrological features of Cement Creek, the upper Animas River, and the confluence and downstream mixing zone have been described by Schemel et al. (2000, 2006) and Schemel and Cox (2005). Discharges in these streams are highest in late spring and decline during the summer months to lowest annual values in late summer and early fall. During this low-discharge period, the upper Animas River typically contributes about 3/4 of the total discharge to the confluence (Schemel et al., 2000). Channel movements in the Animas

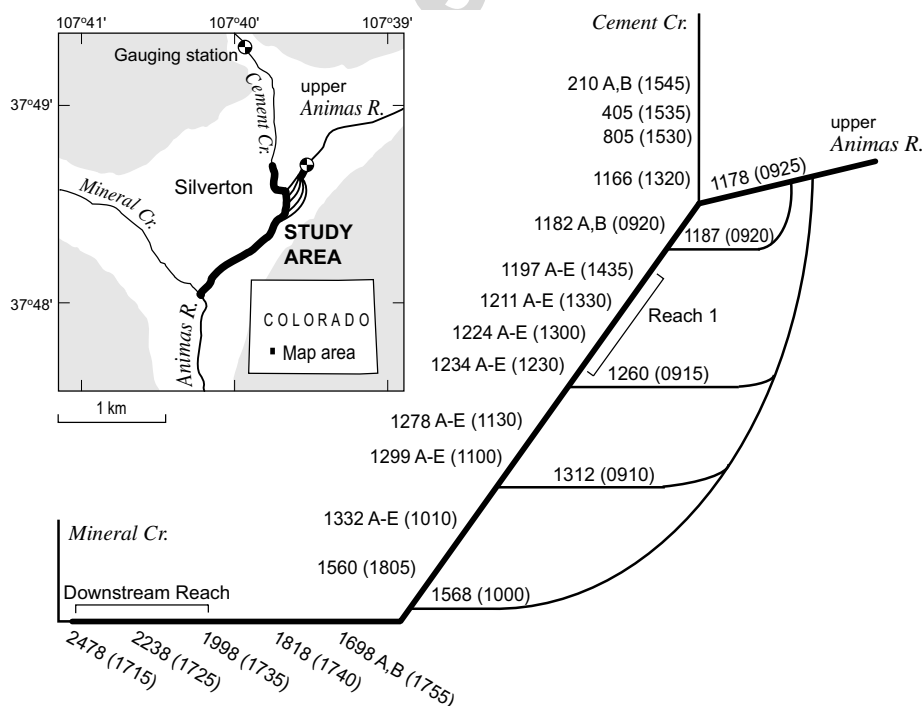


Fig. 1. Map showing Cement Creek and Mineral Creek confluences with the Animas River and locations of discharge gauges near Silverton, Colorado, and diagram showing details of the study area, including sampling sites and sampling times (in parenthesis). Sites where multiple stations were sampled across the channel are shown by A, B (2 stations) and A-E (5 stations). Shaded areas on the map represent surrounding high-elevation mountains of the Silverton caldera.

River floodplain produce significant year-to-year changes in the way the two streams mix when flows are lowest in late summer. In the present study (1997), more braids distributed flow from the Animas River over the first 400 m of the (1300 m) mixing zone than during the 1996 study (Schemel and Cox, 2005). The distribution of inflow in 1997 produced substantial across-channel gradients in chemical concentrations and more-gradual mixing and neutralization of the Cement Creek inflow (Schemel et al., 2006).

3. Methods

The area studied in late summer 1997 included the upper Animas River and Cement Creek downstream from the USGS discharge gauges, the main river channel where the two streams progressively mixed, and the downstream reach, where the river was well mixed upstream from the confluence with Mineral Creek (Fig. 1). In the following text, the collective term, mixing zone, refers to all sites downstream from the confluence of Cement Creek with the first braid (site 1178) of the upper Animas River. Site numbers refer to distance (m) from a reference point in Cement Creek located 145 m downstream from the gauge. Detailed information on the sampling strategy, across-channel field measurements, analytical methods, and the calculation and assignment of mixing ratios to the samples can be found in Schemel et al. (2006). A brief overview is provided here.

3.1. Sample collection and processing

Water samples were collected at sites in Cement Creek and the upper Animas River (source waters) and at sites located within the mixing zone (Fig. 1). One or two samples were collected at sites where the stream appeared to be well mixed. This included sites in Cement Creek, the upper Animas River, and the downstream reach of the mixing zone. Five samples were collected at seven sites where large across-channel differences in specific conductance indicated substantial gradients in chemical composition. The five sampling stations at each site were located at equal increments of specific conductance, as determined by measuring values across the stream with a portable meter. The purpose of this strategy was to obtain samples with a wide range of mixing ratios (see below) representative of the across-channel gradients. An incremen-

tal discharge was estimated for each station using current velocity and depth measured across the stream at each site. Discharge values used in calculations were measured at the sites, obtained from the gauges on the upper Animas River and Cement Creek, or estimated by differences between gauge and site values.

All samples were collected over a 9 h period and processed within about 2 h of the sampling times shown in Fig. 1. Each sample was collected with a vertically integrating sampler using plastic bottles and nozzles that were pre-cleaned with dilute HNO_3 and rinsed with sample water at each station. Samples were kept cool and in the dark before processing. After shaking briefly, whole (W) samples were decanted for metal analyses and for specific conductance and pH, which were measured with portable meters at the field processing site. The remainder of each sample was filtered with a tangential-flow filtration apparatus using $0.45\ \mu\text{m}$ polycarbonate membranes (F filtrates) and 10 k Dalton (approx. $0.001\ \mu\text{m}$ pore size) regenerated cellulose membranes (U filtrates). The filtration apparatus was cleaned with dilute HNO_3 and rinsed with $18.2\ \text{M}\Omega$ deionized water between samples. All samples for metal analyses were acidified with ultrapure HNO_3 (1% final acid concentration).

3.2. Analytical methods

Whole samples (W) were filtered through $0.45\ \mu\text{m}$ capsule filters after digestion in 1% HNO_3 for 1 month or more. In addition, most samples for metals were diluted with 1% ultrapure HNO_3 (by up to a factor of 4 based on their specific conductance values) prior to analysis. This improved the performance of the analyzer and reduced the range of the analytical values. W, F and U filtrates were analyzed for Al, Fe, and Zn using a radial-view Thermo Jarrel Ash inductively coupled plasma-optical emission spectrometer (ICP-OES; any use of trade, product, or firm names is for descriptive purposes only and does not constitute endorsement by the US Government). Aliquots of W and F filtrates were archived and subsequently analyzed for Cu on a more-sensitive ICP-OES instrument with axial-view capabilities.

Analytical values (not adjusted for dilution factors) for most samples fell within the following ranges for Al ($0.1\text{--}1.2\ \text{mg L}^{-1}$), Fe ($0.3\text{--}1.7\ \text{mg L}^{-1}$), Zn ($0.2\text{--}0.4\ \text{mg L}^{-1}$), and Cu ($6\text{--}12\ \mu\text{g L}^{-1}$). Coefficients of variation (CV; standard deviation

divided by the mean) for analyses of reference standards during the analytical runs were 0.016 for Al and Fe, 0.033 for Zn and 0.043 for Cu. The mean values were within 4% of the most probable values for Al and Zn, and within 7% for Fe. For Cu, recoveries of standard additions were 92% at $5 \mu\text{g L}^{-1}$ and greater than 96% for $10 \mu\text{g L}^{-1}$ additions over a $10\text{--}50 \mu\text{g L}^{-1}$ range. Blanks were typically low for Al, Fe and Zn, but were greater relative to the much lower concentrations of Cu. W, F and U filtrates were analyzed sequentially to minimize effects of analytical errors on colloid concentrations, which were estimated by difference. Typically, small differences important for assessing partitioning were reproducible when they were $>0.02 \text{ mg L}^{-1}$ for Zn and $>1 \mu\text{g L}^{-1}$ for Cu.

Dissolved Fe speciation (Fe^{2+} , Fe^{3+}) was measured on F filtrates using the colorimetric bipyridine method, as described by Skougstad et al. (1979). Reagents were added to the filtrates at the field laboratory and absorbances were measured on a spectrophotometer within 2 days.

All chemical concentrations and discharges measured during the field study are available in a data supplement (Cox and Schemel, 2007).

3.3. Laboratory experiments

Mixing experiments using source waters from Cement Creek and the upper Animas River were used to provide additional information on colloid formation and metal sorption in the mixing zone. In general, the experiments were designed to produce mixtures with different proportions of Al and Fe hydrous oxides (HAO and HFO, respectively) over a range of pH, which would allow the relative importance of these sorbents in the dissolved-to-colloidal partitioning of Cu and Zn to be evaluated. The terms, HAO and HFO, are used in the following text with the understanding that both represent a range of possible compositions and can contain variable amounts of SO_4 (Bigham and Nordstrom, 2000).

Fresh source waters were collected for experiments involving Fe, and these experiments were conducted at the field-based laboratory. Some experiments that did not involve Fe used archived source waters that had been filtered and refrigerated in the dark. All source waters had been collected during the late summers of subsequent years, and there were potentially significant differences between the chemistries of the source waters used in the

experiments and those in 1997 even though the discharge conditions were comparable. Concentrations of dissolved Al and Fe are low in the upper Animas River, and most of the Al and Fe that forms colloidal sorbent is from Cement Creek (Schemel et al., 2000). In experiments where HAO was the primary sorbent, Fe^{2+} in the Cement Creek water was allowed to oxidize in the dark near pH 4, which required about 3 days. All of the HFO was then removed by tangential-flow filtration before mixtures were created with ($0.45 \mu\text{m}$) filtered upper Animas River water.

Source waters were proportioned by weight to prepare each bulk sample with a specific mixing ratio, which in some cases was split into individual samples (see below). Samples were placed on a reciprocating shaker for 24 h after mixing. Final pH was determined at $15 \text{ }^\circ\text{C}$, which was near the water temperature in the mixing zone. For each sample, a whole sample (W) was decanted and an aliquot was filtered (F) through a $0.45 \mu\text{m}$ capsule filter. W and F samples were acidified (1% HNO_3), and W samples were filtered after digestion for a few weeks. W and F filtrates were diluted based on their mixing ratios prior to analysis by ICP-OES.

Although laboratory experiments were performed over ranges of mixing ratios, the results presented here are limited primarily to 4 sets of 70% Animas River (AR) mixtures. One sample from each set was a simple mixture of the source waters, and additional samples were amended with small aliquots of HCl to reduce the pH of the mixtures by about 1 pH unit. The sets were: (1) whole-sample mixtures of fresh source waters (Whole); (2) mixtures where all Fe^{2+} had been oxidized at low pH in the Cement Creek water before the source waters were mixed (Lo-pH Fe); (3) mixtures where HFO was removed from fresh Cement Creek water before the source waters were mixed and the remaining Fe^{2+} oxidized and formed colloids at high pH (Hi-pH Fe); and (4) mixtures where all Fe was removed from Cement Creek water before the source waters were mixed (Al only).

3.4. Calculations

Values of the mixing ratio, expressed here as the fraction of water from the upper Animas River (%AR), were assigned to each sample collected in mixing zone ($n = 44$). The assigned mixing ratio was the median of 7 calculated values based on mass balances and concentrations of conservative solutes

(Ca, Mg, Na, Si, Sr, Cl, SO₄) in the samples, Cement Creek, and the upper Animas River (Schemel et al., 2006). Although calculated values for the 7 solutes from each sample were typically comparable within analytical uncertainty, the median value was used to reduce the influence of occasional outliers.

Mass-flow values (kg d⁻¹) for selected sites were calculated from concentrations of Al, Fe, Cu and Zn in the W and F filtrates and measured or estimated discharges (Cox and Schemel, 2007). At the sites in the mixing zone where discrete samples were collected at five stations across the stream, total and dissolved mass-flow values were calculated for each station and the site values were the sums of the station values.

Sorption of Cu and Zn onto HFO was simulated using the surface complexation approach of Dzombak and Morel (1990) as implemented within MINTEQA2 (Allison et al., 1991). Prior to performing the simulations, the thermodynamic database of MINTEQA2 was revised to be consistent with the wateq4f database distributed with PHREEQC (Parkhurst and Appelo, 1999). The mass of sorbent for each sample was based on the observed amount of colloidal Fe as determined by differences between W and F analyses. Sorption parameters (i.e., specific surface area, sorbent molecular weight, low affinity site density) were set using the best estimates of Dzombak and Morel (1990). The high affinity site density was set equal to the upper value reported by Dzombak and Morel (0.01 moles per mole) to reflect the high sorptive capacity of freshly precipitated HFO produced in AMD systems compared to that produced under laboratory conditions (Runkel et al., 1999; Runkel and Kimball, 2002). The set of measured chemical concentrations from each field sample (Cox and Schemel, 2007) was used in the simulations.

Uses of simulations from the sorption model were limited to comparisons with the authors' results in Section 5. An enhanced database for MINTEQA2 (Paulson, 1996) or a similar model (Lofts and Tipping, 1998) could have been used to simulate sorption by both HAO and HFO. These models assume additive sorption, and typically show that sorption by HAO is a small fraction of that for an equivalent amount of HFO. However, HAO and HFO interact, and an additive model might not account for the fundamental changes in surface properties and other factors that control sorption in mixtures. Instead of using an additive

model, the authors chose to evaluate sorption in the natural mixtures using the approach of Anderson and Benjamin (1990a,b), in which (enhanced or inhibited) sorption properties of the mixtures were identified by comparison to sorption by HFO alone. Since the laboratory procedures could not prepare natural mixtures with HFO alone, sorption by HFO was simulated with the MINTEQA2 model, which is often utilized in studies of natural systems.

4. Results

Field results are presented in the following order to (1) quantify source waters (end-members) and the transport of Al, Fe, Cu and Zn through the mixing zone; (2) show effects of mixing on pH and concentrations of dissolved and colloidal metals in the mixing zone, and (3) identify chemical transformations and the partitioning of metals between dissolved and colloidal phases. Results from laboratory studies, which primarily provide additional information on Cu partitioning, follow the field results.

4.1. Field results

Concentrations of total and dissolved Al, Fe, Cu and Zn and pH values for the upper Animas River and Cement Creek and in the downstream reach, where the river was well mixed (sites 1998-2478; Fig. 1), are shown in Table 1. Concentrations from F filtrates were used for the dissolved values because U filtrates were not available for Cu, and because results from F filtrates were not greatly different from U-filtrate values for Al, Fe and Zn in most cases. Of 53 samples collected in the streams and the mixing zone, only 7 for Al and 2 for Fe had differences between F- and U-filtrate values greater than 0.1 mg L⁻¹, and only 5 for Zn had differences greater than 0.02 mg L⁻¹. The median differences between F- and U-filtrate values were 0.01 mg L⁻¹ or less for Al and Zn, but that for Fe was 0.04 mg L⁻¹ and F-filtrate values for 36 of the Fe samples were greater than U-filtrate values by 0.02 mg L⁻¹ or more. These differences, however, represented a small fraction of the total Fe in most cases (see below).

Although inflow from the Animas River was distributed among 5 braids over the upper 400 m of the 1300 m mixing zone, ranges in concentrations of Al, Fe, Cu and Zn among the braids were small in most cases (Table 1). Total concentrations in the Animas

Table 1

Concentrations of total and dissolved (0.45 μm filtrate) Al, Fe, Zn and Cu, and pH in the upper Animas River (median and range of 5 braids), Cement Creek (site 1166), and the downstream reach (median and range of sites 1998, 2238, and 2478)

| Analyte/fraction | Upper Animas River | | Cement Creek | Downstream reach | |
|-----------------------------------|--------------------|-------------|--------------|------------------|-------------|
| | Median | (Range) | Site 1166 | Median | (Range) |
| Al total (mg L^{-1}) | 0.07 | (0.06–0.07) | 4.94 | 1.12 | (1.11–1.14) |
| Al dissolved | 0.03 | (0.03–0.04) | 4.68 | 0.04 | (0.03–0.06) |
| Fe total (mg L^{-1}) | 0.27 | (0.24–0.33) | 6.67 | 1.70 | (1.68–1.75) |
| Fe Dissolved | 0.05 | (0.04–0.06) | 2.90 | 0.30 | (0.27–0.35) |
| Zn total (mg L^{-1}) | 0.40 | (0.40–0.41) | 0.65 | 0.44 | (0.44–0.45) |
| Zn dissolved | 0.38 | (0.37–0.39) | 0.63 | 0.38 | (0.38–0.39) |
| Cu total ($\mu\text{g L}^{-1}$) | 5.2 | (4.2–5.7) | 45 | 14.2 | (14.0–14.5) |
| Cu dissolved | 3.1 | (3.0–3.3) | 42 | 4.6 | (4.6–4.8) |
| pH | 7.55 | (7.52–7.61) | 4.11 | 6.99 | (all 6.99) |

River braids were the lowest measured in this study. Concentrations of total Al, Fe and Cu were substantially higher in Cement Creek; however, the concentration difference between the Animas River and Cement Creek was less than a factor of two for Zn (Table 1). Concentrations measured at 3 upstream sites in Cement Creek (4 samples) were within 7% (Al, Cu and Zn) and 10% (Fe, except for one outlier) of the values at site 1166, even though samples were collected over 2.5 h (Fig. 1). Aluminum, Cu and Zn were mostly dissolved in Cement Creek, whereas only about a half of the total Fe was dissolved. Ferrous iron accounted for more than 86% of the dissolved Fe at all four sites in Cement Creek. Most of the Al and Fe in the Animas River braids was colloidal, but about 60% of the Cu was dissolved and Zn was primarily dissolved.

The difference in pH between (acidic) Cement Creek and the upper Animas River was 3.5 units (Table 1). The pH values near 7 in the downstream reach indicated that the acidic inflow was effectively neutralized in the mixture containing 78% Animas River water (dilution of the Cement Creek inflow by a factor of 4.5). The large change in pH between Cement Creek and the downstream reach alone indicated the potential importance of many chemical reactions involving dissolved and colloidal metals that were identified previously in this mixing zone (Schemel et al., 2000). In addition, visible evidence of chemical reactions in the mixing zone included opalescence caused by the formation of colloids in the water column and colored precipitates on the streambed (Schemel and Cox, 2005).

Total discharge through the mixing zone was $2.2 \text{ m}^3 \text{ s}^{-1}$ ($1.75 \text{ m}^3 \text{ s}^{-1}$ for the upper Animas River and $0.49 \text{ m}^3 \text{ s}^{-1}$ for Cement Creek), but inflows from the river and creek both decreased about 7% over the 9 h sampling period. Mass-flow estimates for total and dissolved metals were examined over two reaches of the mixing zone, Reach 1, encompassing four sites (1197–1234), and the downstream reach (three sites: 1998–2478; Fig. 1). Reach 1, which received inflows from Cement Creek and two braids of the Animas River, had substantial gradients in chemical concentrations across the channel at all four sites (Schemel et al., 2006). Based on measured inflows, the mean mixing ratio for Reach 1 was 40%AR. The mass-flow values for total metals at the sites in Reach 1 were close to the total inputs from the streams, indicating that total metals were transported through this reach without significant losses or gains (Table 2). This was also the case for dissolved metals, with the exception of Al and to a much lesser extent Cu, where lower dissolved mass-flow values indicated net losses of dissolved metals due to formation of or partitioning to colloids without decreases in total metals. Discharges to Reach 1 supplied >90% of the total inputs of Al and Fe to the entire mixing zone, but they accounted for 76% of the Cu and only 44% of the Zn. Therefore, the remaining 3 braids of the Animas River, which contributed 81% of the total inflow from the upper Animas River, supplied <10% of Al and Fe, but were significant sources of Cu and Zn (24% and 56%, respectively).

Discharges from Cement Creek and all 5 braids of the upper Animas River were well mixed at the three sites in the downstream reach, which were

Table 2

Cement Creek and upper Animas River inputs of total (Tot.) and dissolved (Dis.) Fe, Al, Zn and Cu, and high (hi.) and low (lo.) mass-flow values (kg d^{-1}) for sites in two reaches of the mixing zone

| | | Fe | | Al | | Zn | | Cu | |
|---|-----|------|------|------|------|------|------|------|------|
| | | Tot. | Dis. | Tot. | Dis. | Tot. | Dis. | Tot. | Dis. |
| Total of inputs upstream of site 1197 | | 292 | 125 | 212 | 200 | 39 | 38 | 2.06 | 1.87 |
| <i>Reach 1</i> | | | | | | | | | |
| Range of mass-flows for sites 1197–1234 | lo. | 275 | 125 | 202 | 132 | 37 | 36 | 1.99 | 1.64 |
| | hi. | 302 | 136 | 216 | 149 | 38 | 37 | 2.17 | 1.86 |
| Range of %Trans. for sites 1197–1234 | lo. | 95 | 100 | 96 | 66 | 95 | 95 | 97 | 88 |
| | hi. | 103 | 109 | 102 | 75 | 97 | 97 | 103 | 99 |
| Total of inputs upstream of site 1998 | | 325 | 130 | 221 | 204 | 88 | 85 | 2.70 | 2.26 |
| <i>Downstream Reach</i> | | | | | | | | | |
| Range of mass flows for sites 1998–2478 | lo. | 320 | 51 | 212 | 7 | 83 | 72 | 2.68 | 0.88 |
| | hi. | 335 | 67 | 219 | 11 | 86 | 75 | 2.77 | 0.92 |
| Range of %Trans. for sites 1998–2478 | lo. | 98 | 39 | 96 | 3 | 94 | 85 | 99 | 39 |
| | hi. | 103 | 52 | 99 | 5 | 98 | 88 | 103 | 41 |

Transport through each reach (%Trans.) is the ratio of the mass-flow value to the total input ($\times 10^2$). Dis. values are based on FA filtrates.

used to assess transport through the entire mixing zone. Travel time from the confluence of Cement Creek with the first braid of the Animas River to the downstream reach was approximately 40 min, as estimated by the arrival time of the injected tracer (Schemel et al., 2006). Mass-flow values for the downstream reach indicated that stream inputs of total Al, Fe, Cu and Zn were transported through the mixing zone without significant losses (Table 2). In addition, there was no indication of additional sources of these metals, such as groundwater inflow. However, mass-flow estimates for the dissolved metals indicated a small but measurable decrease in dissolved Zn (av. 14%) and large decreases in dissolved Al (>95%), Fe (>48%) and Cu (>59%). Estimates for dissolved Fe based on U filtrates indicated greater losses ranging from 62% to 74% over the three sites. However, the mean difference between the F- and U-filtrate results represented only about 5% of the total Fe mass flow.

In examining results from the mixing zone, plots using the mixing ratio, %AR, were used because linear distributions of concentrations indicate conservative transport through the mixing zone, and distinctly non-linear distributions could indicate chemical reactivity, losses to the streambed, or additional sources (Paulson, 1997; Schemel et al., 2006). Samples collected in the mixing zone using the strategy based on equal increments of specific conductance across the channel covered a wide range of %AR, and the results were distributed adequately over the total range. Over the range of 20–80%AR

each 20% interval contained 10 or more values (total of 34 samples for the 3 intervals, representing 77% of the data). Fewer samples (total of 10) were collected at %AR values less than 20% and greater than 80%. Reactions involving hydrolysis, precipitation, and sorption are more directly related to pH than the mixing ratio. However, plots using the mixing ratio are perhaps more useful in this particular case because they clearly show the effects of dilution. In addition, pH increased in a consistent manner with increasing values of %AR over much of this mixing zone (Fig. 2). Ranges of pH are specified where needed to describe relevant processes in the following text.

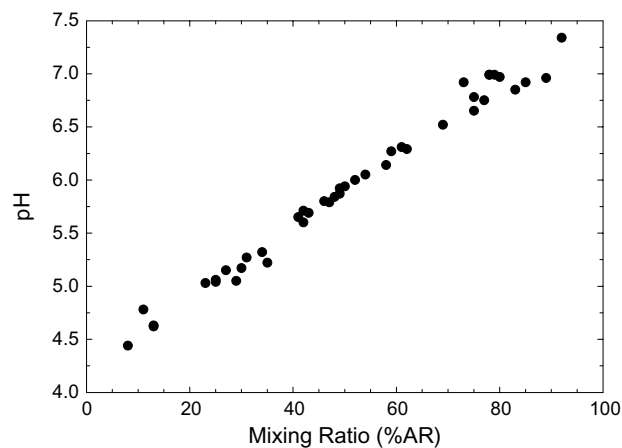


Fig. 2. Plot of pH versus the mixing ratio (%AR) for samples collected at sites in the mixing zone.

Mixing plots showing concentrations of total, dissolved, and colloidal (by difference) Al and Fe are shown in Fig. 3. For both Al and Fe, total concentrations were linearly distributed relative to %AR and were located close to (theoretical) conservative mixing lines based on concentrations in the end members (Table 1). Conservative transport of both total Al and total Fe indicated by the mixing plots was consistent with the mass-flow estimates, which showed negligible losses of these metals through the study area.

Nearly all of the Al, which was mostly dissolved in Cement Creek, had been transformed to colloids in the (well-mixed) downstream reach (Table 2). Fig. 3 shows details of this transformation, which was predictable from the increase in pH that accompanied the dilution of Cement Creek water by the Animas River. Nearly all of the dissolved Al partitioned to the colloidal fraction between pH 4.8 and 6.5, which was consistent with the precipitation of HAO (Nordstrom and Ball, 1986). In addition to

samples from the downstream reach, all samples with $\text{pH} > 6.5$ had concentrations of dissolved Al $< 0.1 \text{ mg L}^{-1}$ regardless of location in the mixing zone.

Ferrous iron averaged 97% of the dissolved Fe and accounted for 40–50% of the total Fe in samples with mixing ratios less than about 65%AR, which corresponded to a sample pH of about 6.5 (Fig. 4). Colloidal Fe was a significantly higher fraction (70–95%) of the total Fe in the downstream reach and in other samples where pH and %AR values were higher. Therefore, oxidation of dissolved Fe^{2+} and precipitation of colloidal HFO was most evident at pH values that were higher than the pH range (4.8–6.5) where most HAO was formed. The relative (mole fraction) abundances of HAO and HFO varied over the range of the mixing ratio and pH (Fig. 5). Some HFO was supplied directly to the mixing zone by Cement Creek, but HAO became equally abundant (by mole) as it precipitated in the 5.0–5.5 pH range. Continued precipitation of HAO made it more abundant than HFO by about a factor of two in the 5.5–6.5 pH range, but increased oxidation and precipitation of Fe at higher pH reduced the difference.

Zinc concentrations in the mixing zone were more than a factor of 10 greater than Cu concentrations (Fig. 6). Dilution of Cement Creek by the upper Animas River had a large effect on Cu concentrations, but the effect of mixing on Zn concentrations was much smaller. Concentrations of total Zn and Cu clustered about their respective conservative mixing lines, indicating that losses through the mixing zone were relatively small, as also shown by the mass-flow estimates (Fig. 6; Table 2). Forma-

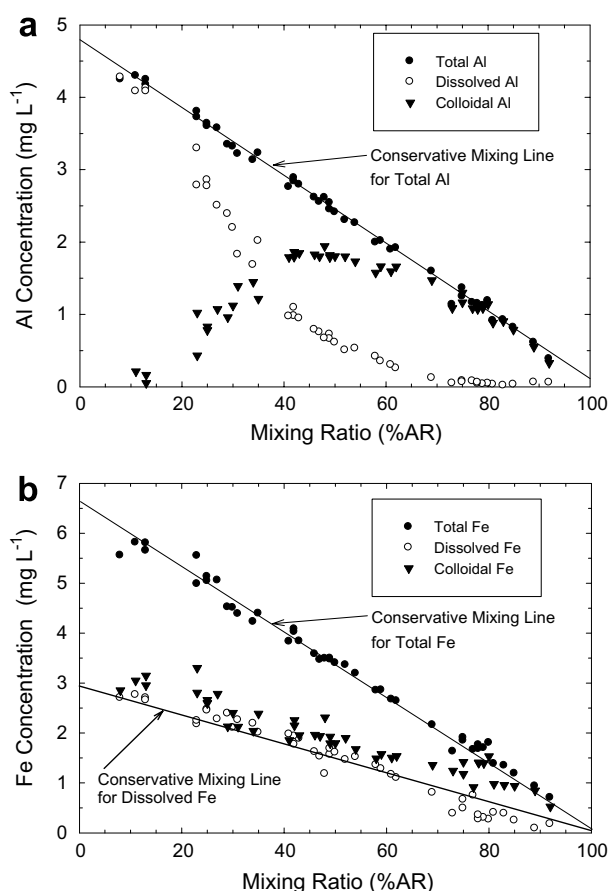


Fig. 3. Total, dissolved and colloidal Al (a) and Fe (b) versus the mixing ratio (%AR) for samples collected at sites in the mixing zone.

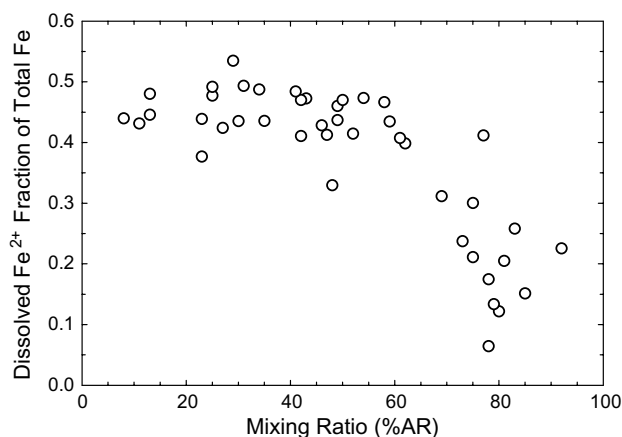


Fig. 4. Dissolved Fe^{2+} fraction of the total Fe versus the mixing ratio (%AR) for samples collected at sites in the mixing zone.

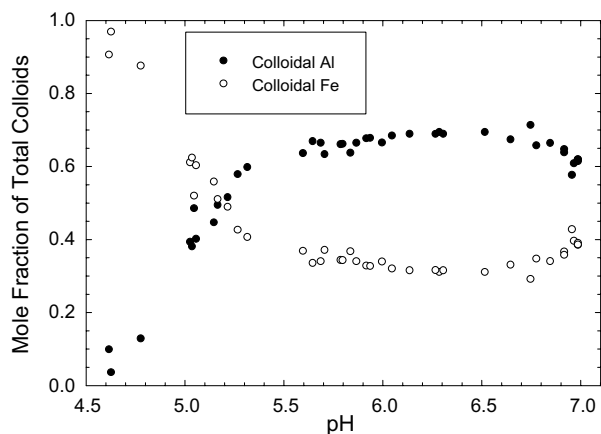


Fig. 5. Colloidal Al and Fe mole fractions of the total colloids versus pH for samples collected at sites in the mixing zone.

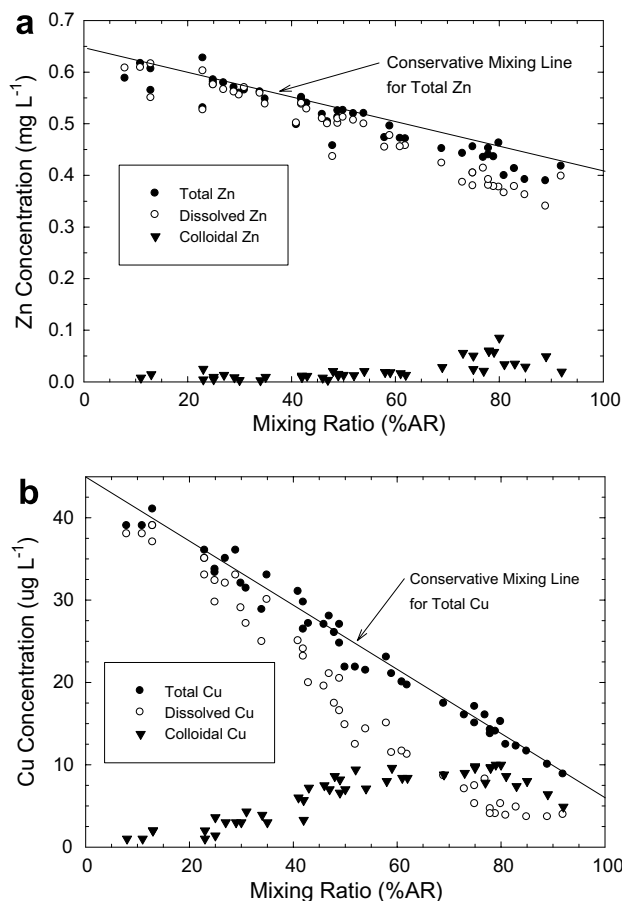


Fig. 6. Total, dissolved and colloidal Zn (a) and Cu (b) versus the mixing ratio (%AR) for samples collected at sites in the mixing zone.

tion of colloidal Zn was significant only at $\text{pH} > 6.5$, which was predominantly in the downstream reach of the mixing zone, where colloidal Zn averaged 14% of the total Zn. In contrast, colloidal Cu was clearly detectable above $\text{pH} 5$ and reached a maxi-

imum fraction of the total Cu (60–70%) near $\text{pH} 7$. Even though a small fraction of the total Zn was colloidal, there was typically more colloidal Zn than colloidal Cu (by mole) at circumneutral pH in the downstream reach (see below).

4.2. Laboratory results

Mixing experiments with varying fractions (%AR) of source waters produced general patterns of dissolved-to-colloidal partitioning similar to those exhibited by the field samples (results not shown). Like the field samples, these experiments showed effects of pH -dependent reactions as well as effects of the dilution of HFO and HAO sorbents and Cu and Zn sorbates. Consequently, it was difficult to isolate the effects of any one factor, such as the increase in pH . In these experiments, Fe^{2+} in the Cement Creek source water was allowed to oxidize and form HFO, and then the sample was split into two sets. For one set of mixtures HFO was removed by filtration, and only HAO was formed when mixed with upper Animas River source water. Both HFO and HAO were produced in the other (unfiltered) set. The fraction (%) of the total Cu that was colloidal (%Col.Cu) increased with pH in both sets of mixtures; however %Col.Cu values were greater for mixtures containing both HFO and HAO. For example, the set containing both sorbents reached the 50%Cu (sorbed) level at a pH about 0.5 unit lower than the set with only HAO. A small fraction of the total Zn (<10%) was colloidal in these mixing experiments and in the experiments described below, and the analytical precision was not sufficient to distinguish differences between the different sorbent mixtures.

Experiments with a single mixture, 70%AR, were conducted to identify differences in Cu partitioning relative to sorbent composition without the additional effects of dilution. Four sets of samples were prepared as described in Methods (Whole, lo.- pH Fe, hi.- pH Fe, Al only). Differences in the compositions of the samples resulted from variability in source waters, sample preparation, and final pH . Final pH values ranged from 7.12 to 7.26 for unamended samples of the 4 sets, whereas the pH values of samples amended with small amounts of HCl were lower by as much as 1 pH unit (Table 3). Most of the Al and Fe was colloidal (HAO, HFO) in samples with $\text{pH} > 7$, whereas as much as a third of the total Al and Fe remained dissolved in the samples near $\text{pH} 6.3$. The range in total Cu among the sam-

Table 3
Concentrations of colloidal (Col.) Al, Fe and Cu and total (Tot.) Cu, and the mole fraction of Col. Fe to total Col

| Sample set Final pH | Col. Al (mg L ⁻¹) | Col. Fe (mg L ⁻¹) | Mole Fraction Col. Fe:Col.Al+Fe | Col. Cu (μg L ⁻¹) | Tot. Cu (μg L ⁻¹) |
|------------------------|----------------------------------|----------------------------------|------------------------------------|----------------------------------|----------------------------------|
| <i>Lo-pH Fe</i> | | | | | |
| 6.31 | 1.37 | 2.14 | 0.431 | 13.9 | 34.6 |
| 7.24 | 1.65 | 2.17 | 0.389 | 22.6 | 34.9 |
| <i>Whole</i> | | | | | |
| 6.37 | 1.39 | 1.52 | 0.346 | 10.7 | 35.3 |
| 7.13 | 1.66 | 1.89 | 0.355 | 21.1 | 34.8 |
| <i>Hi-pH Fe</i> | | | | | |
| 6.32 | 1.45 | 1.00 | 0.250 | 8.4 | 36.6 |
| 7.12 | 1.81 | 1.48 | 0.283 | 19.0 | 36.3 |
| <i>Al only</i> | | | | | |
| 6.32 | 1.51 | 0 | 0 | 5.9 | 32.2 |
| 6.39 | 1.56 | 0 | 0 | 7.1 | 32.5 |
| 6.57 | 1.63 | 0 | 0 | 9.2 | 31.2 |
| 6.58 | 1.58 | 0 | 0 | 8.3 | 31.5 |
| 6.95 | 1.70 | 0 | 0 | 12.2 | 31.5 |
| 7.26 | 1.77 | 0 | 0 | 16.1 | 30.4 |

Al + Fe in samples from the laboratory experiments with 70%AR mixes.

ples was 15% of the mean value, which was small compared to the ranges for HAO (27% of the mean) and HFO (69% of the mean for the 6 samples containing HFO). HAO was more concentrated than HFO in all of the samples, and differences among the samples produced a range of the HFO mole fraction (of the total HAO plus HFO) from 0 to 0.431 (Table 3).

Data from the experiments are summarized in Fig. 7, in which colloidal Cu is shown as the fraction (%Col.) of the total Cu. Final pH values for samples

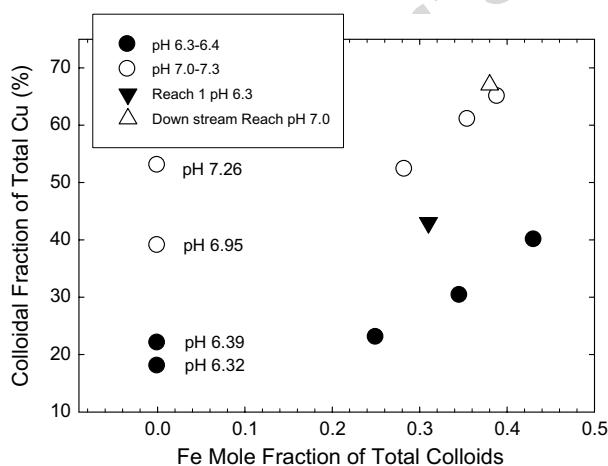


Fig. 7. Colloidal fraction of the total Cu versus the Fe mole fraction of the total colloids for laboratory experiments (data from Table 3) and samples collected in Reach 1 and the Downstream Reach (mean of 3 samples from each location).

that contained HAO alone (0 Fe mole fraction) show that a pH increase of one unit produced an increase in the %Col.Cu by a factor of two, while the corresponding increase in HAO was only 17% (Table 3). For samples that contained both HAO and HFO, %Col.Cu increased with the increase in Fe mole fraction and Cu sorption was significantly greater over the higher pH range. This trend was also indicated by field samples collected in Reach 1 (pH 6.3–6.4) and the downstream reach (pH 7.0), which showed greater values of %Col.Cu at the higher Fe mole fraction and pH in the downstream reach (Fig. 7). Experimental results in Fig. 7 also indicate that Cu sorption with HFO in the mixtures was not much greater than that for HAO alone when the mole fraction of HFO was low. Data in Table 3 indicated that the presence of HFO with HAO resulted in greater partitioning of Cu (per mole relative to HAO alone) by a factor of 1.3–2.1 near pH 6.3, but the additional partitioning of Cu per mole of HFO was about the same as that for HAO in the higher pH range.

5. Discussion

This section begins with a comparison of field results from this study with those made during the previous study. Next, variability in the mixed sorbent composition and the relative effects of dilution on concentrations are discussed. Finally, field and

laboratory observations are combined with MINT-EQA2 model simulations of sorption. Sorption of Zn is considered first because previous laboratory studies have described Zn sorption by HAO–HFO mixtures (Anderson and Benjamin, 1990a,b).

5.1. Comparison of results from the 1996 and 1997 studies

Field results from 1997 confirmed observations made during the 1996 study (Schemel et al., 2000) and provided additional detail on the formation of colloids and new data on Cu partitioning and transport. Total discharge through the mixing zone and total concentrations of Al, Fe and Zn in the upper Animas River and Al and Fe in Cement Creek were similar between the two years, but total Zn was less concentrated in Cement Creek in 1997. Consequently, mass flows through the mixing zone were nearly the same in both years for Al and Fe, and the range of values in 1997 was 9–14% lower for Zn. Total and dissolved Cu were not measured in 1996, but the estimated mass flow through the mixing zone for colloidal Cu in 1996 (1.8 kg d^{-1}) was within the range of values in 1997.

Although some precipitate was visible on the streambed in both years (Schemel and Cox, 2005), mass flows of total Al, Fe and Zn through the mixing zone were not significantly lower than the combined inputs from Cement Creek and the upper Animas River during both studies. This was also the case for total Cu in 1997. Consequently, interactions with or losses to the streambed were not as important for these metals as dilution and chemical transformations in the water column as they were transported through the mixing zone. Furthermore, these results suggest that dissolved-to-colloidal partitioning of Cu and Zn should primarily involve HAO and HFO in the water column. Discharge levels and channel geometry indicated minimal contact time with the streambed in most of the mixing zone (Schemel et al., 2006), and newly formed suspended colloids might be more effective sorbents than older, more-crystalline precipitates accumulated on the streambed (Hrncir and McKnight, 1998; Smith et al., 1998).

5.2. Chemical transformations and dilution

HAO was produced in the mixing zone, but HFO was both supplied by Cement Creek and formed by oxidation of Fe^{2+} (and precipitation of Fe^{3+}) in the

mixing zone. HFO from Cement Creek accounted for a large fraction (72%) of the total HFO in the downstream reach because only about half of the dissolved Fe^{2+} load had oxidized during transport through the mixing zone. Samples collected in the downstream reach were not filtered on site. Instead, they were processed within 2 h after collection, which was longer than the travel time through the entire mixing zone (approx. 40 min). Processing time allowed for further oxidation, which suggests that the HFO supplied by Cement Creek was an even greater fraction of the total in the downstream reach. HFO supplied by Cement Creek and that newly formed in the mixing zone could have different compositions and properties. Precipitation in the low-pH, high- SO_4 waters of Cement Creek would form minerals that contain more SO_4 compared to hydrolysis products formed under conditions in the downstream reach (Bigham et al., 1996). In addition, HFO from Cement Creek was probably a mixture of colloids formed in the streamflow and particles resuspended from the streambed, which could be larger and more crystalline depending on their age. HFO from Cement Creek would likely become coated as HAO precipitated in the mixing zone. The formation of new HFO in the mixing zone, however, was significant only at $\text{pH} > 6.5$, which is higher than the range where HAO was formed. Although laboratory studies indicate that this newly formed HFO would also become coated with HAO over time (Anderson and Benjamin, 1990a), it is not known to what extent HAO affected the properties of HFO produced within the mixing zone.

Competition between two processes, the oxidation of Fe^{2+} and the photoreduction of dissolved Fe^{3+} and newly formed HFO, also could influence the composition of the mixed sorbent in the mixing zone. In general, photoreduction is most significant in acidic waters, and oxidation is more important than photoreduction at circumneutral pH (McKnight et al., 2001; Gammons et al., 2005). Consequently, conditions in the downstream reach favor the net production of HFO, as was observed.

In addition to neutralization and chemical transformations, dilution was an important factor influencing concentrations of the mixed HAO–HFO sorbent and therefore the dissolved-colloidal partitioning of Cu and Zn. Nearly all of the Al and Fe was supplied by Cement Creek, and mixing with Animas River water lowered concentrations of the colloids available to sorb metals particularly in the

downstream reach (dilution factor of 4.5). Although concentrations of Cu were also substantially diluted, decreases in Zn concentrations were minimal because of the much smaller difference between the two streams. As a result, Zn maintained high concentrations throughout the mixing zone while dilution lowered concentrations of the mixed sorbent and increased the ratio of sorbate to sorbent (see below). Although laboratory neutralization of AMD-affected streamflow is commonly used to identify relevant processes and products that can be formed (e.g., Munk et al., 2002; Lee et al., 2002; Jönsson et al., 2006), the present results show that effects of dilution cannot be ignored in studies of natural confluences where concentrations of sorbents or sorbates can be greatly affected.

5.3. Dissolved-colloidal partitioning of Zn and Cu

Zinc and Cu can be sorbed by both HAO and HFO. Copper is sorbed at a lower pH than Zn by both sorbents, and equivalent sorption of each metal occurs at a lower pH with HFO compared to HAO (Kinniburgh et al., 1976). HFO is typically the stronger sorbent for cations. This has been shown for Zn in laboratory studies of sorption by synthetic HAO and HFO, both independently and with mixtures of these two sorbents (Anderson and Benjamin, 1990a). In the present laboratory experiments with natural source waters, the experimental methods could produce Cement Creek-Animas River mixtures with HAO alone and with both HAO and HFO, but could not produce samples with only natural HFO. Consequently, the MINTEQA2 model was utilized to simulate (predict) sorption of Zn and Cu by HFO alone for comparisons between laboratory and field results in the following discussion. Relative to the results, it was expected that the model predictions would be lower if the presence of HAO contributed to additional sorption, whereas model predictions would be higher if the presence of HAO inhibited sorption by HFO.

As mentioned above, the upper value suggested for high-affinity site density was used in the simulations to account for enhanced sorption properties of naturally formed HFO in the simulations (0.01 versus the “best estimate” value, 0.005 moles per mole). Increasing the surface complexation constants is an alternative approach proposed recently in other studies of AMD systems with high SO_4 (Swedlund and Webster, 2001) or high sorbate-to-

sorbent ratios (Tonkin, 2002; Balistrieri et al., 2003). The effects of increasing the high-affinity site density and using an alternative set of constants (Tonkin, 2002) were evaluated (relative to using “best estimate” values) for 4 test samples with pH ranging from 5.22 to 6.85. For Cu, the effect of increasing high-affinity site density was nearly identical to the effect of increasing the constants over the pH range of 5.87 (39% increase) to 6.85 (<4% increase). Differences were greater at pH 5.22, where increasing the high-affinity site density resulted in a 71% increase and increasing the constants increased sorption by a factor of two. Results for Zn showed that increasing the high-affinity site density increased sorption by nearly a factor of two in the pH range of 5.22–6.31, but differences were smaller at pH 6.85 (43% increase). In contrast, increasing the constants resulted in increased sorption of Zn by factors of 3–5 over the entire pH range, with the greatest increases occurring at the highest pH. These tests suggest that the model used below (with the upper value for high-affinity site density) should yield results similar to a model using increased constants above pH 5.87 for Cu, but that increased constants produce much greater sorption than the model used in this study for Zn over the entire pH range.

Laboratory and modeling studies by Anderson and Benjamin (1990a,b) have shown that interactions of HFO and HAO in binary mixtures enhance the sorption of Zn and that sorption increases as the proportion of HAO to HFO increases. Although they identified many factors that might have contributed to this effect, their results were consistent with the formation of an HAO coating on the HFO. In addition to a significant change in the surface properties of the HFO, the HAO reduced the sizes of HFO particles and increased the surface area of the mixed sorbent. This included the disaggregation of previously formed HFO particles. In addition to contributing to enhanced sorption of Zn, the reduction in particle size could have important implications for the HFO that formed in Cement Creek and then moved through the mixing zone. If HAO–HFO interactions reduced particle sizes or limited aggregation, this could, in part, contribute to the minimal losses of total Al and Fe to the streambed in the mixing zone.

Field values for (%) colloidal Zn were generally 2–4 times greater than model predictions in the 5.5–7.0 pH range (Fig. 8), which might be more than expected from the enhanced sorptive properties of

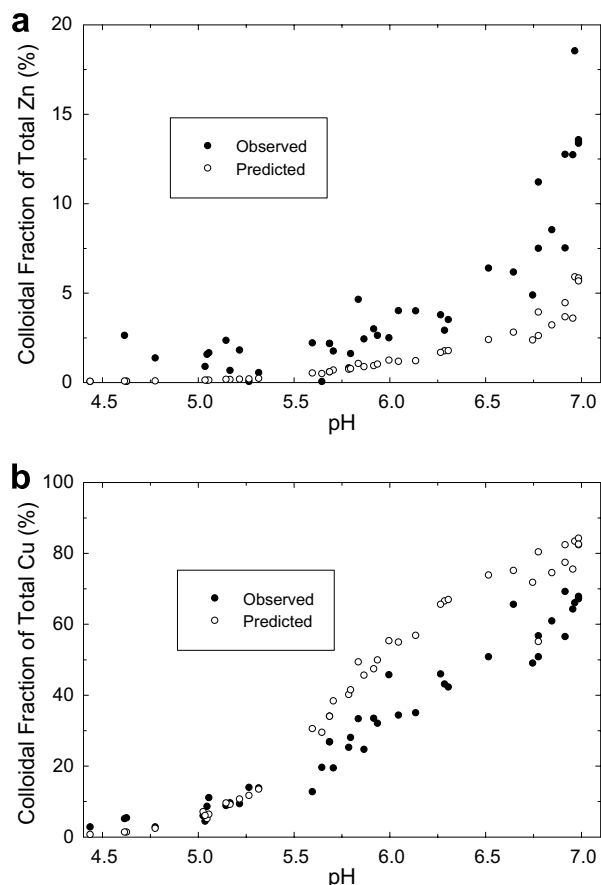


Fig. 8. Colloidal fraction of the total Zn (a) and total Cu (b) for field samples and predicted values from the MINTEQ2A model versus pH.

the mixed sorbent (Anderson and Benjamin, 1990a). However, the methods used in this study were reliable for measuring colloidal Zn only at concentrations greater than about $20 \mu\text{g L}^{-1}$, which corresponds to the $\text{pH} > 6.5$ range where additional HFO was being formed. Concentrations of total Zn were high relative to concentrations of the colloids in this high pH range (mole ratio of total sorbate:sorbent of 0.27 for HFO and 0.17 for HAO in the downstream reach). There are several reasons why greater colloidal Zn concentrations might be expected than would be predicted by the model at such high sorbate:sorbent ratios. Tonkin (2002) has suggested that high ratios require the use of increased values for surface complexation constants used by the model. However, simulations using the increased constants for samples from the mixing zone with $\text{pH} > 6.5$ predicted colloidal Zn concentrations that were even greater than those observed by an average of 74%.

Sorption of Zn might be enhanced by many factors in this mixing zone, and processes such as

coprecipitation with HFO as it is forming or surface precipitation also should be considered. Crawford et al. (1993) found that preformed HFO sorbed an equivalent amount of Zn compared to HFO formed in the presence of Zn, indicating that simple coprecipitation was not a likely process. However, X-ray adsorption extended fine structure spectroscopy (EXAFS) has provided more-detailed information on the speciation of sorbed Zn. Characterization of Zn sorbed by ferrihydrite over a range of Zn concentrations showed that the formation of Zn hydroxide polymers was enhanced on the HFO surface at high sorbate:sorbent ratios (>0.2 ; Waychunas et al., 2002). In addition, a possible contribution by HAO was suggested by an EXAFS study in which Zn–Al hydroxide coprecipitates formed on colloidal Al (Trainor et al., 2000). Although mixtures of HAO and HFO can exhibit properties that are different from the individual components, surface polymers or Zn–Al coprecipitates that can form at high sorbate:sorbent ratios could help explain why the amounts of colloidal Zn in the field samples exceeded predictions from the model.

A greater fraction of the total Cu was colloidal compared to Zn (Fig. 8), as might be expected from their total concentrations and because Cu sorbs onto both HFO and HAO at lower pH than Zn. Lower total Cu concentrations also resulted in lower Cu sorbate:sorbent ratios (e.g., 0.009 for HFO and 0.005 for HAO in the downstream reach). At these levels, the increased constants proposed by Tonkin (2002) might not be appropriate, although tests suggested that there would be relatively small differences in predictions compared to the model used in this study. Predictions of Cu sorption were similar to observed (%) colloidal Cu values over the 5.0–5.3 pH range (Fig. 8), where field values were sufficiently large relative to analytical uncertainty and HFO averaged 50% of the total colloids (Fig. 5). However, model predictions were consistently higher than the field results (47% average) over the 5.6–6.8 pH range (Fig. 8), where HAO was enriched in most samples by a factor of two (Fig. 5). Most predictions for these samples decreased to within $\pm 25\%$ of the field values when the high-affinity site density was reduced to 0.005 moles per mole, which could indicate that naturally formed HFO in the HAO-rich mixture was not as strong a sorbent as would be expected. The value for high-affinity site density did not have a large effect on predictions for samples in the 6.8–

7.0 range, where most values were within $\pm 25\%$ of the field results regardless of the site-density value. Although mixtures in this pH range were still HAO-rich, formation of new HFO reduced the difference compared to the 5.6–6.8 pH range (Fig. 5). Perhaps the most important conclusion from these model and field results is that the sorption of Cu by the HAO-rich mixture did not appear to be greater than was expected for HFO alone, and there are indications that it might be less.

Model simulations with data from the experiments containing both HAO and HFO (Table 3) also over predicted concentrations of colloidal Cu. Experimental results were 47–57% of the model predictions in the 6.3–6.4 pH range, which were in general agreement with results from the field study. The laboratory experiments showed that HAO alone could sorb a substantial fraction of the Cu, but that sorption was even greater as the mole fraction of HFO increased. However, the results also indicated that additional HFO did not produce substantial sorption over HAO alone when the mole fraction of HFO was low (Fig. 7). This was particularly evident in the data from the 6.3–6.4 pH range, where only a small increase in sorbed Cu was observed when the HFO mole fraction increased from 0 to 0.25, and the effect of increasing HFO appeared greatest at the highest mole fraction. These observations from the experiments were generally consistent with the model and field results, in that Cu sorption was closest to expected values in the downstream reach, where new HFO had increased the HFO mole fraction (pH > 6.8).

Although interaction of HAO and HFO and changes in their fundamental properties when mixed could be affecting the sorption of Cu and Zn, other factors possibly contribute to differences between field results and model predictions in this chemically complex natural system. The model assumed that all of the HFO was newly formed, which could lead to overestimates if the HFO from Cement Creek contained a substantial fraction of older and more crystalline particles. However, HFO formed in Cement Creek is more likely to contain SO_4 than HFO formed at higher pH in the mixing zone, and Cement Creek is also a large source of SO_4 to the mixing zone (Schemel et al., 2000, 2006; Kimball et al., 2002). Sorption of Cu and Zn onto HFO can be enhanced by dissolved SO_4 or SO_4 within the mineral structure (Ali and Dzombak, 1996; Webster et al., 1998; Swedlund and Webster, 2001). Significant effects of SO_4 , however, are lim-

ited to low pH and low sorbate:sorbent ratios (generally < 0.005 ; Swedlund and Webster, 2001). Consequently, the presence of SO_4 or SO_4 -rich HFO might not be expected to be dominant factors affecting sorption of Cu or Zn in this mixing zone. Likewise, SO_4 can be associated with HAO (Nordstrom, 1982) or the sorbent mixture formed in the mixing zone, but its influence on sorption of Cu and Zn also might not be significant at high pH.

In general, streams that drain the Silverton caldera have low concentrations of dissolved organic C (DOC), although it is expected that some organic matter is also associated with particles. The authors' unpublished measurements indicate that concentrations of DOC in the mixing zone were probably in the range of 0.2–0.6 mg L^{-1} , which is comparable to measurements in the river downstream. Copper can form strong complexes with organic ligands present in natural DOC. In general, organic complexation enhances the sorption of Cu to both HAO and HFO at low pH, but can reduce sorption at circumneutral pH by the formation of soluble complexes (Davis and Leckie, 1978; Davis, 1984). Although laboratory and field studies have shown that Zn sorption onto HAO and HFO can be enhanced by fulvic acid, formation of soluble complexes at high pH appears to be less important than for Cu (McKnight et al., 1992; Düker et al., 1995; Zuyi et al., 2000). About 60% of the total Cu was dissolved in the upper Animas River (pH 7.6) and possibly complexed by organic and inorganic ligands (Sunda and Hanson, 1979). Calculations using the Windermere Humic Aqueous Model (WHAM; Tipping, 1994; Lofts and Tipping, 1998) estimated that about a half of the total Cu could be complexed if most of the DOC (0.4 mg L^{-1}) was fulvic acid. A similar WHAM calculation for the downstream reach, where the Animas River supplied 41% of the total Cu, showed that 0.4 mg L^{-1} DOC could reduce colloidal Cu concentrations by about 25%.

In contrast to the results from this study with HAO-rich sorbent, Cu sorption has been underestimated by models in many studies involving both HFO alone and HFO-rich mixed sorbents (e.g., Runkel et al., 1999; Karthikeyan and Elliott, 1999; Tonkin et al., 2002; Balistrieri et al., 2003). Surface precipitation can substantially increase partitioning of Cu to both HAO and HFO at circumneutral pH, but this probably was not significant at the low sorbate:sorbent ratios in the downstream reach (Karthikeyan et al., 1999; Karthikeyan and Elliott,

1999). In general, HFO is a stronger sorbent than HAO for Cu at low sorbent:sorbate ratios, particularly when the HFO is being formed in solution with Cu (Karthikeyan et al., 1997, 1999). The field results and model estimates for Cu sorption showed the best agreement (within 25%) and the greatest (%) Cu sorption at pH > 6.8 (e.g., the downstream reach), where HFO was being formed and might not have been affected by colloidal HAO that had formed at lower pH. Therefore, it appears likely that the formation of new HFO at circumneutral pH was a primary factor contributing to greater Cu sorption in the downstream reach.

6. Conclusions

In this study, detailed sampling within the mixing zone identified chemical transformations associated with the neutralization and dilution of inflow from a metal-enriched creek by a circumneutral river. Significant observations that could apply in studies of similar natural confluences are summarized below:

1. In addition to differences in the effects of dilution on total concentrations, all four metals showed different degrees of chemical transformation from dissolved to colloidal form. Formation of, or partitioning to, colloids was greatest for Al and least for Zn.
2. The increase in pH as the acidic inflow was neutralized was a major factor affecting the formation of HAO and HFO and, in turn, the composition of the mixed sorbent. HFO was supplied to the mixing zone, but the HAO that formed as pH increased from 4.8 to 6.5 produced a mixed sorbent that was enriched in HAO by a factor of two. When pH exceeded 6.5, oxidation of Fe²⁺ formed new HFO and reduced this difference.
3. The partitioning of Cu and Zn to the colloids was also pH dependent. Copper partitioning was evident at a much lower pH than that for Zn, but both metals exhibited greatest partitioning at circumneutral pH, coinciding with the formation of new HFO. The fraction of the total concentration that was colloidal at circumneutral pH was greater for Cu, but more moles of Zn were colloidal due to its higher concentration.
4. Laboratory studies have investigated the sorption properties of HAO–HFO mixed sorbents (compared to HFO alone) for Zn. Although the present comparisons of field and model results

support (previously shown) greater Zn sorption in the HAO–HFO mixtures, the high sorbate-to-sorbent ratio in this natural system indicated the potential importance of additional, surface-related processes.

5. Comparisons of field and model results for Cu indicated that the natural mixed sorbent did not produce more sorption than would be expected for HFO alone, but this might be a result of a combination of factors in this natural system rather than directly related to properties of the mixed sorbent.

Experimental studies, such as those conducted with Zn by Anderson and Benjamin (1990a), that also employ EXAFS or similar techniques (Waychunas et al., 2002; Trainor et al., 2000), could clarify the effects of HAO–HFO mixtures on Cu sorption. Other aspects of mixed-sorbent formation and changes in physical and chemical properties might be worth additional investigation, including effects on particle size.

Acknowledgements

The field study depended on a large number of participants who laid out the sampling transects, made stream measurements, collected water samples, and processed the samples in the field laboratory. We greatly appreciate all of their help, but personally acknowledge R.E. Broshears, J.B. Evans, M.A. Mast, K. Walton-Day and T.J. Yager. We appreciate comments on the manuscript and suggestions from L.S. Ballistrieri, C.C. Fuller, and two anonymous reviewers. This research was funded by the USGS Toxic Substances Hydrology Program Abandoned Mines Initiative and the National Research Program.

References

- Ali, M.A., Dzombak, D.A., 1996. Interactions of copper, organic acids, and sulfate in goethite suspensions. *Geochim. Cosmochim. Acta* 60, 5045–5053.
- Allison, J.D., Brown, D.S., Novo-Gradac, K.J., 1991. MINT-EQA2/PRODEFA2, A geochemical assessment model for environmental systems: Version 3.0 user's manual. US Environmental Protection Agency Report EPA/600/3-91/021.
- Anderson, P.R., Benjamin, M.M., 1990a. Surface and bulk characteristics of binary oxide suspensions. *Environ. Sci. Technol.* 24, 692–698.
- Anderson, P.R., Benjamin, M.M., 1990b. Modeling adsorption in aluminum–iron binary oxide suspensions. *Environ. Sci. Technol.* 24, 1586–1592.

- Baars, D.L., 1992. The American Alps: the San Juan Mountains of Southwest Colorado. University of New Mexico Press, Albuquerque.
- Balistrieri, L.S., Box, S.E., Tonkin, J.W., 2003. Modeling precipitation and sorption of elements during mixing of river water and porewater in the Coeur d'Alene River Basin. *Environ. Sci. Technol.* 7, 4694–4701.
- Berger, A.C., Bethke, C.M., Krumschl, J.L., 2000. A process of natural attenuation in drainage from a historic mining district. *Appl. Geochem.* 15, 655–666.
- Bigham, J.M., Nordstrom, D.K., 2000. Iron and aluminum hydroxysulfates from acid sulfate waters. In: Alpers, C.N., Jambor, J.C., Nordstrom, D.K. (Eds.), *Sulfate minerals, crystallography, geochemistry, and environmental significance*, Reviews in Mineralogy and Geochemistry, 40. Mineralogical Society of America, Washington, DC, pp. 351–403 (Chapter 7).
- Bigham, J.M., Schwertmann, U., Pfab, G., 1996. Influence of pH on mineral speciation in a bioreactor simulating acid mine drainage. *Appl. Geochem.* 11, 845–849.
- Bove, D.J., Hon, K., Budding, K.E., Slack, J.F., Snee, L.W., Yeoman, R.A., 2001. Geochronology and geology of late Oligocene through Miocene volcanism and mineralization in the Western San Juan Mountains, Colorado. US Geological Survey Prof. Paper 1642.
- Chapman, B.M., Jones, D.R., Jung, R.F., 1983. Processes controlling metal ion attenuation in acid mine drainage streams. *Geochem. Cosmochim. Acta* 47, 1957–1973.
- Church, S.E., Kimball, B.A., Fey, D.L., Ferderer, D.A., Yager, T.J., Vaughn, R.B., 1997. Source, transport and partitioning of metals between water, colloids, and bed sediments of the Animas River, Colorado. US Geological Survey Open-File Report 97-151.
- Coston, J.A., Fuller, C.C., Davis, J.A., 1995. Pb^{2+} and Zn^{2+} adsorption by a natural aluminum- and iron-bearing surface coating on an aquifer sand. *Geochim. Cosmochim. Acta* 59, 3535–3547.
- Cox, M.H., Schemel, L.E., 2007. Chemical and hydrologic data from the Cement Creek and upper Animas River confluence and mixing zone, Silverton, Colorado, September 1997. US Geological Survey Open-file Report 2007-1048. <<http://pubs.usgs.gov/of/2007/1048/>>.
- Crawford, R.J., Harding, I.H., Mainwaring, D.E., 1993. Adsorption and coprecipitation of single heavy metal ions onto the hydrated oxides of iron and chromium. *Langmuir* 9, 3050–3056.
- Davis, J.A., 1984. Complexation of trace metals by adsorbed natural organic matter. *Geochim. Cosmochim. Acta* 48, 679–691.
- Davis, J.A., Leckie, J.O., 1978. Effect of adsorbed complexing ligands on trace metal uptake by hydrous oxides. *Environ. Sci. Technol.* 2, 1309–1315.
- Davis, J.A., Coston, J.A., Kent, D.B., Fuller, C.C., 1998. Application of the surface complexation concept to complex mineral assemblages. *Environ. Sci. Technol.* 32, 2820–2828.
- Dinelli, E., Tateo, F., 2002. Different types of fine-grained sediments associated with acid mine drainage in the Libiola Fe–Cu mine area (Ligurian Apennines, Italy). *Appl. Geochem.* 17, 1081–1092.
- Düker, A., Ledin, A., Karlsson, S., Allard, B., 1995. Adsorption of zinc on colloidal (hydr)oxides of Si, Al and Fe in the presence of a fulvic acid. *Appl. Geochem.* 10, 197–205.
- Dzombak, D.A., Morel, F.M., 1990. *Surface Complexation Modeling: Hydrous Ferric Oxide*. Wiley, New York.
- Fox, L.E., 1988. The solubility of colloidal ferric hydroxide and its relevance to iron concentrations in river water. *Geochem. Cosmochim. Acta* 52, 771–777.
- Gammons, C.H., Nimick, D.A., Parker, S.R., Cleasby, T.E., McCleskey, R.B., 2005. Diel behavior of iron and other heavy metals in a mountain stream with acidic to neutral pH: Fisher Creek, Montana, USA. *Geochim. Cosmochim. Acta* 69, 2505–2516.
- Hrncir, D.C., McKnight, D., 1998. Variation in photoreactivity of iron hydroxides taken from an acidic mountain stream. *Environ. Sci. Technol.* 32, 2137–2141.
- Jönsson, J., Jönsson, J., Löugren, L., 2006. Precipitation of secondary Fe(III) minerals from acid mine drainage. *Appl. Geochem.* 21, 437–445.
- Karthikeyan, K.G., Elliott, H.A., 1999. Surface complexation modeling of copper sorption by hydrous oxides of iron and aluminum. *J. Colloid Interface Sci.* 220, 88–95.
- Karthikeyan, K.G., Elliott, H.A., Cannon, F.S., 1997. Adsorption and coprecipitation of copper with the hydrous oxides of iron and aluminum. *Environ. Sci. Technol.* 31, 2721–2725.
- Karthikeyan, K.G., Elliott, H.A., Chorover, J., 1999. Role of surface precipitation in copper sorption by the hydrous oxides of iron and aluminum. *J. Colloid Interface Sci.* 209, 72–78.
- Khare, N., Hesterberg, D., Martin, J.D., 2005. XANES investigation of phosphate sorption in single and binary systems of iron and aluminum oxide minerals. *Environ. Sci. Technol.* 39, 2152–2160.
- Kimball, B.A., Runkel, R.L., Walton-Day, K., Bencala, K.E., 2002. Assessment of metal loads in watersheds affected by acid mine drainage by using tracer injection and synoptic sampling: Cement Creek, Colorado, USA. *Appl. Geochem.* 17, 1183–1207.
- Kimball, B.A., Walton-Day, K., Runkel, R.L., 2007. Quantification of metal loading by tracer injection and synoptic sampling, 1996–2000. In: Church, S.E., von Guerard, P., Finger, S.E. (Eds.), *Integrated investigations of environmental effects of historical mining in the Animas River watershed, San Juan County, Colorado*. US Geological Survey Prof. Paper 1651 (Chapter E9).
- Kinniburgh, D.G., Jackson, M.L., Syers, J.K., 1976. Adsorption of alkaline earth, transition, and heavy metal cations by hydrous oxide gels of iron and aluminum. *Soil Sci. Soc. Am. J.* 40, 796–799.
- Lee, G., Bigham, J.M., Faure, G., 2002. Removal of trace metals by coprecipitation with Fe, Al, and Mn from natural waters contaminated with acid mine drainage in the Ducktown Mining District, Tennessee. *Appl. Geochem.* 17, 569–581.
- Lipman, P.W., Fisher, W.S., Mehnert, H.H., Naeser, C.W., Luedke, R.G., Steven, T.S., 1976. Multiple ages of mid-Tertiary mineralization and alteration in the western San Juan Mountains, Colorado. *Econ. Geol.* 71, 571–588.
- Lofts, S., Tipping, E., 1998. An assemblage model for cation binding by natural particulate matter. *Geochim. Cosmochim. Acta* 62, 2609–2625.
- McKnight, D.M., Wershaw, R.L., Bencala, K.E., Zellweger, G.W., Feder, G.L., 1992. Humic substances and trace metals associated with Fe and Al oxides deposited in an acidic mountain stream. *Sci. Total Environ.* (117/118), 485–498.
- McKnight, D.M., Kimball, B.A., Runkel, R.L., 2001. pH dependence of iron photoreduction in a rocky mountain

- stream affected by acid mine drainage. *Hydrol. Process* 15, 1979–1992. doi:10.1002/hyp.251.
- Meng, X., Letterman, R.D., 1993. Effect of component oxide interaction on the adsorption properties of mixed oxides. *Environ. Sci. Technol.* 27, 970–975.
- Munk, L., Faure, G., Pride, D.E., Bigham, J.M., 2002. Sorption of trace metals to an aluminum precipitate in a stream receiving acid rock-drainage; Snake River, Summit County, Colorado. *Appl. Geochem.* 17, 421–430.
- Nordstrom, D.K., 1982. The effect of sulfate on aluminum concentrations in natural waters: some stability relations in the system $\text{Al}_2\text{O}_3\text{--SO}_3\text{--H}_2\text{O}$ at 298 K. *Geochim. Cosmochim. Acta* 46, 681–692.
- Nordstrom, D.K., Alpers, C.N., 1999. Geochemistry of acid mine waste. In: Plumlee, G.S., Logsdon, M.J. (Eds.), *The environmental geochemistry of mineral deposits—reviews in economic geology*, vol. 6A. Society of Economic Geologists, Littleton, CO, pp. 133–160.
- Nordstrom, D.K., Ball, J.W., 1986. The geochemical behavior of aluminum in acidified surface waters. *Science* 232, 54–56.
- Parkhurst, D.L., Appelo, C.A., 1999. User's Guide to PHREEQC (Version 2) – a computer program for speciation, batch-reaction, and one-dimensional transport, and inverse geochemical calculations, US Geological Survey Water Resources Investigation Report, 1999, 99-4259.
- Paschke, S.S., Kimball, B.A., Runkel, R.L., 2005. Quantification and simulation of metal loading to the upper Animas River, Eureka to Silverton, San Juan County, Colorado, September 1997 and August 1998. US Geological Survey Scientific Investigation, Report 2005-5054. <<http://pubs.usgs.gov/sir/2005/5054/>>.
- Paulson, A.J., 1996. Fate of Metals in Surface Waters of the Coeur d'Alene Basin, Idaho. US Bureau of Mines. Report of Investigations 9620.
- Paulson, A.J., 1997. The transport and fate of Fe, Mn, Cu, Zn, Cd, Pb, and SO_4 in a groundwater plume and in downstream surface waters in the Coeur d'Alene Mining District, Idaho, USA. *Appl. Geochem.* 12, 447–464.
- Ranville, J.F., Schmiermund, R.L., 1999. General aspects of aquatic colloids in environmental chemistry. In: Plumlee, G.S., Logsdon, M.J. (Eds.), *The environmental geochemistry of mineral deposits – reviews in economic geology*, vol. 6A. Society of Economic Geologists, Littleton, CO, pp. 183–199 (Chapter 8).
- Runkel, R.L., Kimball, B.A., 2002. Evaluating remedial alternatives for an acid mine drainage stream: application of a reactive transport model. *Environ. Sci. Technol.* 36, 1093–1101.
- Runkel, R.L., Kimball, B.A., McKnight, D.M., Bencala, K.E., 1999. Reactive solute transport in streams: a surface complexation approach for trace metal sorption. *Water Resour. Res.* 35, 3829–3840.
- Schemel, L.E., Cox, M.H., 2005. Descriptions of the Cement Creek-Animas River confluence and mixing zone near Silverton, CO, during 1996 and 1997. US Geological Survey Open-file Report 2005-1064. <<http://pubs.usgs.gov/of/2005/1064/>>.
- Schemel, L.E., Kimball, B.A., Bencala, K.E., 2000. Colloid formation and metal transport through two mixing zones affected by acid mine drainage near Silverton, Colorado. *Appl. Geochem.* 15, 1003–1018.
- Schemel, L.E., Kimball, B.A., Runkel, R.L., Cox, M.H., 2006. Multiple injected and natural conservative tracers quantify mixing in a stream confluence affected by acid mine drainage near Silverton, Colorado. *Hydrol. Process.* 20, 2727–2743. doi:10.1002/hyp.6081.
- Singer, P.C., Stumm, W., 1970. Acid mine drainage: the rate-determining step. *Science* 167, 1121–1123.
- Skougstad, M.W., Fishman, M.J., Friedman, L.C., Erdmann, D.E., Duncan, S.S., 1979. Methods for Determination of Inorganic Substances in Water and Fluvial Sediments. US Geological Survey Techniques of Water Resources Investigations, Book 5, pp. 373–374.
- Smith, K.S., 1999. Metal sorption on mineral surfaces: an overview with examples relating to mineral deposits. In: Plumlee, G.S., Logsdon, M.J. (Eds.), *The environmental geochemistry of mineral deposits – reviews in economic geology*, vol. 6A. Society of Economic Geologists, Littleton, CO, pp. 161–182 (Chapter 7).
- Smith, K.S., Ranville, J.F., Plumlee, G.S., Macalady, D.L., 1998. Predictive double-layer modeling of metal sorption in mine-drainage systems. In: Jenne, E.A. (Ed.), *Adsorption of Metals by Geomedia*. Academic Press, pp. 522–544 (Chapter 24).
- Sunda, W.G., Hanson, P.J., 1979. Chemical speciation of copper in river water. In: Jenne, E.A. (Ed.), *Chemical Modeling in Aqueous Systems*. American Chemical Society, Washington, DC, pp. 47–180 (Chapter 8).
- Swedlund, P.J., Webster, J.G., 2001. Cu and Zn ternary surface complex formation with SO_4 on ferrihydrite and schwertmannite. *Appl. Geochem.* 16, 503–511.
- Tipping, E., 1994. WHAMC – a chemical equilibrium model and computer code for waters, sediments, and soils incorporating a discrete site/electrostatic model of ion-binding by humic substances. *Computers Geosci.* 20, 973–1023.
- Tonkin, J.W., 2002. Metal Partitioning in the Aqueous Environment: Field, Laboratory and Modeling Studies. Ph.D. Dissertation, University of Washington.
- Tonkin, J.W., Balistrieri, L.S., Murray, J.W., 2002. Modeling metal removal onto natural particles formed during mixing of acid rock drainage with ambient surface water. *Environ. Sci. Technol.* 36, 484–492.
- Trainor, T.P., Brown Jr., G.E., Parks, G.A., 2000. Adsorption and precipitation of aqueous Zn(II) on alumina powders. *J. Colloid Interface Sci.* 231, 359–372.
- Waychunas, G.A., Fuller, C.C., Davis, J.A., 2002. Surface complexation and precipitate geometry for aqueous Zn(II) sorption on ferrihydrite I: X-ray absorption extended fine structure spectroscopy analysis. *Geochim. Cosmochim. Acta* 66, 1119–1137.
- Webster, J.G., Swedlund, P.J., Webster, K.S., 1998. Trace metal adsorption onto an acid mine drainage iron (III) oxy hydroxy sulfate. *Environ. Sci. Technol.* 32, 1361–1368.
- Yager, D.B., Bove, D.J., 2002. Generalized geologic map of part of the upper Animas River watershed and vicinity, Silverton, Colorado. US Geological Survey Miscellaneous Field Studies Map MF-2377.
- Zuyi, T., Taiwei, C., Jinzhou, D., XiongXin, D., Yingjie, G., 2000. Effect of fulvic acids on sorption of U(VI), Zn, Yb, I and Se(IV) onto oxides of aluminum, iron and silicon. *Appl. Geochem.* 15, 133–139.